H．知的財産権の出願・登録状況

なし.

研究成果の刊行に関する一覧表

雑誌

発表者氏名	論文タイトル名	発表誌名	巻号	ページ	出版年
Shimazaki H, Sakoe K, Niijima K, Nakano I, Takiyama Y	An unusual case of a spasticity-lacking phenotype with a novel *SACS* mutation.	Journal of the Neurological Sciences	255	87-89	2007
Ishikawa T, Morita M. Nakano I	Constant blood flow reduction in premotor frontal lobe regions in ALS with dementia —a SPECT study with 3D-SSP	Acta Neurol Scand	116	340-344	2007
Shimazaki H, Ando Y, Nakano I, Dalmau J	Reversible limbic encephalitis with antibodies against the membranes of neurons of the hippocampus	Journal of Neurology, Neurosurgery and Psychiatry	78	324-325	2007

研究成果の刊行に関する一覧表

雑誌

発表者氏名	論文タイトル名	発表誌名	巻号	ページ	出版年
Nonaka-Sarukawa, M., Okada, T., Ito, T., Yamamoto, K., Yoshioka, T., Nomoto, T., Hojo, Y., Shimpo, M., Urabe, M., Mizukami, H., Kume, A., Ikeda, U., Shimada, K., Ozawa, K.	Adeno-associated virus vector-mediated systemic interleukin-10 expression ameliorates hypertensive organ damage in Dahl salt-sensitive rats.	J Gene Med			*in press*
Liu, Y., Okada, T., Shimazaki, K., Sheykholeslami, K., Nomoto, T., Muramatsu, SI., Mizukami, H., Kume, A., Xiao, S., Ichimura, K., Ozawa, K.	Protection Against Aminoglycoside-induced Ototoxicity by Regulated AAV Vector-mediated GDNF Gene Transfer Into the Cochlea.	Mol Ther			*in press*
Ito, T., Okada, T., Miyashita, H., Nomoto, T., Nonaka-Sarukawa, M., Uchibori, R., Maeda, Y., Urabe, M., Mizukami, H., Kume, A., Takahashi, M., Ikeda, U., Shimada, K., Ozawa, K.	Interleukin-10 expression mediated by an adeno-associated virus vector prevents monocrotaline-induced pulmonary arterial hypertension in rats.	Circ Res	101(7)	734-41	2007
Ito, T., Okada, T., Mimuro, J., Miyashita, H., Uchibori, R., Urabe, M., Mizukami, H., Kume, A., Takahashi, M., Ikeda, U., Sakata, Y., Shimada, K., Ozawa, K.	Adenoassociated virus-mediated prostacyclin synthase expression prevents pulmonary arterial hypertension in rats.	Hypertension	50(3)	531-6	2007

Liu, Y., Okada, T., Nomoto, T., Ke, X., Kume, A. Ozawa, K., and Xiao, S.	Promoter effects of adeno-associated viral vector for transgene expression in the cochlea in vivo.	Exp Mol Med	39(2)	170-175	2007

研究成果の刊行に関する一覧表

書籍

著者氏名	論文タイトル名	書籍全体の編集者名	書 籍 名	出版社名	出版地	出版年	ページ
Muramatsu S	AAV vectors provide a valuable tool for neuroscience.	Pablo S. Ruiz	Genetic vectors research focus	Nova Science Publishers	New York	2007	31-34

雑誌

発表者氏名	論文タイトル名	発表誌名	巻号	ページ	出版年
Sawada H, Hshida R, Hirata Y, Ono K, Suzuki H, Muramatsu S, Nakano I,Nagatsu T, Sawada M	Activated microglia affect the nigro-striatal dopamine neurons differently in neonatal and aged mice treated with 1-methyl-4-phenyl-1,2,3,6-tetrahydropyridine has.	J Neurosci Res	85(8)	1752-1761	2007
Wakamatsu M, Ishii A, Iwata S, Sakagami J,Ukai Y, Ono M, Kanbe D, Muramatsu S, Kobayashi K, Iwatsudo T, Yoshimoto M	Selective loss of nigral dopamine neurons induced by overexpression of truncated human a-synuclein in mice.	Neurobiol Aging			*in press*

研究成果の刊行物・別刷

ELSEVIER

Journal of the Neurological Sciences 255 (2007) 87–89

Journal of the Neurological Sciences

www.elsevier.com/locate/jns

An unusual case of a spasticity-lacking phenotype with a novel *SACS* mutation

Haruo Shimazaki [a], Kumi Sakoe [a], Kenji Niijima [b], Imaharu Nakano [a], Yoshihisa Takiyama [a,*]

[a] *Division of Neurology, Department of Internal Medicine, Jichi Medical University, Yakushiji 3311-1, Shimotsuke, Tochigi 329-0498, Japan*
[b] *Niijima Clinic, Shimotsuke, Tochigi 329-0502, Japan*

Received 29 November 2006; received in revised form 31 January 2007; accepted 1 February 2007

Abstract

The authors describe an unusual case of autosomal recessive spastic ataxia of Charlevoix–Saguenay (ARSACS) without leg spasticity, which is a core clinical feature of ARSACS. This is the second family with a spasticity-lacking phenotype in ARSACS. A peripheral nerve conduction study disclosed decreases in motor and sensory nerve conduction velocities with the disease progression. Although the leg spasticity is reported to become progressively worse during the disease and is prevalent in older patients, we first observed that the symptom had disappeared, probably due to the progressive peripheral nerve degeneration in the disease course. Thus, we should analyze the *SACS* gene even in cases of early-onset cerebellar ataxia without spasticity. The patient had a novel homozygous 2-base pair deletion mutation (c.5988–9 del CT) of the *SACS* gene, but the genotype was different from that in our first family of this phenotype. A further genotype–phenotype correlation study is required to clarify the molecular mechanism underlying 'sacsinopathies'.

Keywords: ARSACS; Deletion mutation; Spasticity; SPECT with 3D-SSP analysis

1. Introduction

Autosomal recessive spastic ataxia of Charlevoix–Saguenay (ARSACS; OMIM 270550) was originally described in families from the Charlevoix–Saguenay region in Quebec, in the northeast of Canada. The clinical phenotype of ARSACS patients in Quebec is uniform, and characterized by early-onset ataxia of gait, progressive spasticity, peripheral neuropathy, normal mentality and retinal striation [1]. In 2000, the gene responsible for ARSACS, *SACS*, was discovered [2]. The open reading frame (ORF) of *SACS* was initially reported to comprise 11,487 bp and to be encoded by a single gigantic exon [2]. In the recent version of Genome Project Gene Predictions, however, eight exons upstream the original *SACS* ORF are indicated and thus the new ORF is 13,737 bp long (http://www.ncbi.nlm.nih.gov/entrez/viewer.fcgi?db=nucleotide&val=13620292). To date, more than 20 mutations have been reported worldwide [3–5].

Recent reports have revealed that ARSACS shows phenotypic variability, e.g., absence of retinal striation [6–9] and presence of mental impairment [9–12]. Furthermore, we previously reported two sibling cases without spasticity elsewhere [13], although we could not determine whether their spasticity had gradually decreased or not existed from the onset of disease. Here we report a case that exhibited a decrease in leg spasticity during the 29-year course of the disease, with a novel *SACS* gene mutation.

2. Methods

We report a patient in a Japanese family with early-onset ataxia. The unaffected elder sister underwent thorough neurological evaluation by H.S. The father and mother were not consanguineous, and had died at ages 82 and 34 years of pulmonary fibrosis and a sarcoma, respectively.

* Corresponding author. Tel.: +81 285 58 7352; fax: +81 285 44 5118.
E-mail address: ytakiya@jichi.ac.jp (Y. Takiyama).

0022-510X/$ - see front matter © 2007 Elsevier B.V. All rights reserved.
doi:10.1016/j.jns.2007.02.002

We performed conventional nerve conduction studies on sensory and motor nerves. Sensory nerves were examined by means of the antidromic stimulation technique.

The patient was examined by means of *N*-isopropyl-*p* [^{123}I] iodoamphetamine (^{123}I-IMP) single photon emission computed tomography (SPECT), and the images obtained were analyzed by means of three-dimensional streotactic surface projection (3D-SSP) using image-analysis software, iSSP, ver. 3.5 (Nihon Medi-Physics).

Blood samples were obtained with informed consent from the patient and her elder sister. Genomic DNA was extracted from peripheral blood leukocytes. Using 38 appropriate primer pairs (all primer sequences are available on request), the coding exons of the *SACS* gene were amplified by PCR from 200 ng of genomic DNA, and then sequenced directly with an ABI PRISM 3100 genetic analyzer; the analysis was performed with Sequencing Analysis software, ver. 5.2 (Applied Biosystems).

This study was approved by the Medical Ethical Committee of Jichi Medical University.

3. Case report

A 57-year-old woman first walked at 3 years. Her gait was unsteady and she could not run in the first decade. She could walk with assistance until 25 years old. She was admitted to our hospital at age 27 years because of slowly progressive gait disturbance in October 1977. Neurological examination at age 27 years revealed mild distal muscle weakness and atrophy of the extremities. She exhibited spasticity in the lower extremities. Her tendon reflexes were exaggerated with the absence of ankle jerks. The Babinski sign was present bilaterally. She showed limb and truncal ataxia with scanning and slurred speech. Her gait was ataxic and spastic. Horizontal gaze-evoked nystagmus was noted. Vibratory sensation in the lower extremities was reduced. She showed claw-hand and hammer-toe deformities, and pes cavus. Myelinated retinal nerve fibers were observed in the retina. A nerve conduction study revealed that motor nerve conduction velocity was mildly reduced and sensory nerve conduction velocity was also reduced except for in the sural nerves, for which no sensory nerve action potential could be evoked (Table 1). Brain CT revealed cerebellar atrophy. A sural nerve biopsy revealed loss of large myelinated fibers (data not shown).

Table 1
Peripheral neurophysiologic study

	Nerve (left)	1977/11/04	2006/01/31	Normal
MCV	Ulnar	48.4	34.8	49–68 m/s
	Median	37.7	NE	47–60 m/s
	Common peroneal	26.8	NE	43–62 m/s
	Posterior tibial	27.0	NE	41–61 m/s
SCV	Ulnar (hand)	24.5	26.4	46–60 m/s
	Median (hand)	36.5	24.9	45–68 m/s
	Sural	NE	NE	34–49 m/s

MCV: motor nerve conduction velocity, SCV: sensory nerve conduction velocity, NE: not evoked.

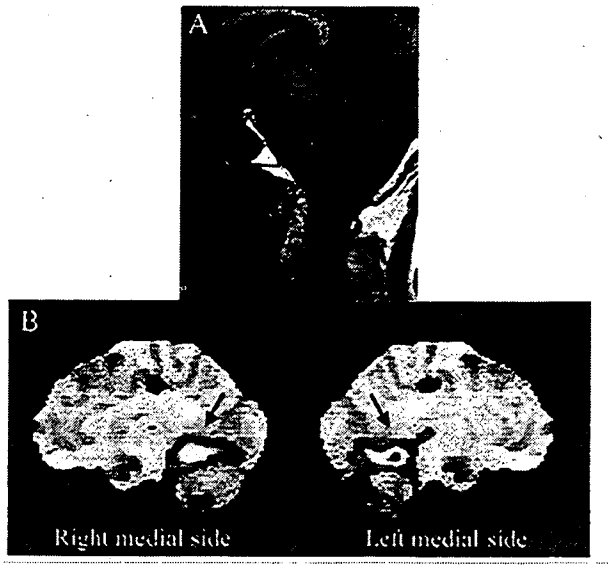

Fig. 1. (A) Brain MRI of the patient. Brain MRI revealed cerebellar superior vermian atrophy without brainstem atrophy. (B) ^{123}I-IMP SPECT with 3D-SSP analysis. The results showed decreased blood flow in the superior cerebellar vermis (arrow) and cerebellar hemisphere.

After discharge, she could walk with a walker, but her gait disturbance gradually progressed and she became wheelchair-bound at age 45. She fell down and developed a subdural hematoma, and thus underwent burrhole irrigation at the same time. Dysphagia emerged at age 54. Neurological examination at age 57 years disclosed the absence of spasticity and moderate muscle weakness in the lower extremities. Her severe limb and truncal ataxia resulted in unsteadiness on sitting on the side of bed. Both superficial and deep sensations were disturbed, especially in the distal parts of the extremities. The tendon reflexes had almost completely disappeared in the upper and lower extremities. The Babinski sign was still present. The leg spasticity was no longer evident, apparently because of progressive motor and sensory neuropathies. A nerve conduction study revealed that motor nerve potentials were not evoked except for in the ulnar nerves and sensory nerve conduction velocity was reduced except for in the sural nerves, for which no sensory nerve action potential could be evoked (Table 1). Brain MRI revealed cerebellar atrophy, especially in the superior vermis (Fig. 1A). ^{123}I-IMP SPECT revealed decreased blood flow in the whole cerebellum (data not shown), whereas SPECT with 3D-SSP analysis showed decreased blood flow in the superior cerebellar vermis (Fig. 1B).

A homozygous 2-base pair deletion mutation, c.5988–9 del CT (GenBank Accession No. AL157766) in exon 9 of the *SACS* gene, was identified in the patient. The elder sister had a heterozygous state of this condition.

4. Discussion

The present patient showed characteristic features of ARSACS, as follows: cerebellar ataxia, peripheral neuropathy, retinal striation, and cerebellar atrophy, especially in the

superior vermis. However, it is noteworthy that our patient lacked leg spasticity, i.e., a core clinical feature of ARSACS. In Quebec and non-Quebec patients, the leg spasticity becomes progressively worse during the disease and is prevalent in older patients, and tendon reflexes remain preserved throughout the disease, except for ankle jerks [1,8]. Meanwhile, we previously reported two brothers with ARSACS without spasticity [13]. In those cases, we were not able to determine whether or not their spasticity had decreased during the disease course or had been absent from the onset, because we only observed them at one time [13]. In the present patient, we observed that leg spasticity and tendon reflexes decreased during the 29-year disease course. This is the second family with ARSACS without spasticity [13], and is the first observation that spasticity and tendon reflexes decreased during the disease course of ARSACS. There is a possibility that severe peripheral nerve degeneration, as indicated by the biopsied sural nerve and peripheral nerve conduction velocities, masked any spasticity. The present patient again indicates that progressive spasticity is not a constant feature of ARSACS [13], and that we should analyze the *SACS* gene even in cases of early-onset cerebellar ataxia without spasticity.

The characteristic MRI findings in ARSACS are cerebellar atrophy, especially in the upper vermis, as shown in our patient, and a small spinal cord in the cervical segment [3]. The MRI findings in 11 of 14 patients with early-onset cerebellar ataxia with retained tendon reflexes (EOCA) reflected marked cerebellar atrophy affecting the upper and lower vermis, and hemispheres to almost the same degree [15]. In Friedreich's ataxia (FA), the MRI findings in all 11 patients reflected upper cervical cord shrinkage, and only one of the 11 patients at an advanced stage showed moderate cerebellar atrophy [15]. Thus, there are some different MRI findings among EOCA, FA, and ARSACS. In the present study, we showed that 3D-SSP analysis on brain SPECT revealed decreased blood flow in the superior cerebellar vermis. This finding might reflect atrophy of the superior cerebellar vermis. To our knowledge, SPECT with 3D-SSP analysis in ARSACS has not been reported so far. Meanwhile, EOCA and FA often show a reduction in the parietotemporal cortex blood flow as well as cerebellar hypoperfusion [14], a different feature from ARSACS. Although we should perform further SPECT analyses in ARSACS, 3D-SSP analysis on brain SPECT could be a useful tool for the differential diagnosis of early-onset cerebellar ataxias in addition to brain and cervical MRI, and gene analysis.

Genetically, the present patient had a novel homozygous deletion mutation (c.5988–9 del CT) of the *SACS* gene, which resulted in a frameshift and a subsequent stop codon at amino acid residue 1999. This mutation leads to truncation of the predicted sacsin protein. However, our first ARSACS family without spasticity had a homozygous missense mutation of the *SACS* gene. Thus, it does not appear that the leg spasticity-lacking phenotype is affected by a certain genotype. Concerning the 2-base pair deletion mutation in the *SACS* gene like our case, there has been only one report with a compound heterozygous state in more than 20 mutations reported [9]. So far, a genotype–phenotype correlation has not been demonstrated in ARSACS. As more *SACS* mutations are identified, a finer genotype–phenotype correlation study will become possible.

Acknowledgements

The authors thank the family for participating in this study. This work was supported by a grant from the Research Committee for Ataxic Diseases (Y.T.) of the Ministry of Health, Labor and Welfare, Japan, and by a Jichi Medical University Young Investigator Award (H.S.).

References

[1] Bouchard JP, Barbeau A, Bouchard R, Bouchard RW. Autosomal recessive spastic ataxia of Charlevoix–Saguenay. Can J Neurol Sci 1978;5:61–9.
[2] Engert JC, Berube P, Mercier J, Dore C, Lepage P, Ge B, et al. ARSACS, a spastic ataxia common in northeastern Quebec, is caused by mutations in a new gene encoding an 11.5-kb ORF. Nat Genet 2000;24:120–5.
[3] Takiyama Y. Autosomal recessive spastic ataxia of Charlevoix–Saguenay. Neuropathology 2006;26:368–75.
[4] Ouyang Y, Takiyama Y, Sakoe K, Shimazaki H, Ogawa T, Nagano S, et al. Sacsin-related ataxia (ARSACS): expanding the genotype upstream from the gigantic exon. Neurology 2006;66:1103–4.
[5] Criscuolo C, Sacca F, De Michele G, Mancini P, Combarros O, Infante J, et al. Novel mutation of *SACS* gene in a Spanish family with autosomal recessive spastic ataxia. Mov Disord 2005;20:1358–61.
[6] Hara K, Onodera O, Endo M, Kondo H, Shiota H, Miki K, et al. Sacsin-related autosomal recessive ataxia without prominent retinal myelinated fibers in Japan. Mov Disord 2005;20:380–2.
[7] Richter AM, Ozgul RK, Poisson VC, Topaloglu H. Private *SACS* mutations in autosomal recessive spastic ataxia of Charlevoix–Saguenay (ARSACS) families from Turkey. Neurogenetics 2004;5: 165–70.
[8] El Euch-Fayache G, Lalani I, Amouri R, Turki I, Ouahchi K, Hung WY, et al. Phenotypic features and genetic findings in sacsin-related autosomal recessive ataxia in Tunisia. Arch Neurol 2003;60:982–8.
[9] Yamamoto Y, Hiraoka K, Araki M, Nagano S, Shimazaki H, Takiyama Y, et al. Novel compound heterozygous mutations in sacsin-related ataxia. J Neurol Sci 2005;239:101–4.
[10] Criscuolo C, Banfi S, Orio M, Gasparini P, Monticelli A, Scarano V, et al. A novel mutation in *SACS* gene in a family from southern Italy. Neurology 2004;62:100–2.
[11] Ogawa T, Takiyama Y, Sakoe K, Mori K, Namekawa M, Shimazaki H, et al. Identification of a *SACS* gene missense mutation in ARSACS. Neurology 2004;62:107–9.
[12] Grieco GS, Malandrini A, Comanducci G, Leuzzi V, Valoppi M, Tessa A, et al. Novel *SACS* mutations in autosomal recessive spastic ataxia of Charlevoix–Saguenay type. Neurology 2004;62:103–6.
[13] Shimazaki H, Takiyama Y, Sakoe K, Ando Y, Nakano I. A phenotype without spasticity in sacsin-related ataxia. Neurology 2005;64: 2129–31.
[14] De Michele G, Mainenti PP, Soricelli A, Di Salle F, Salvatore E, Longobardi MR, et al. Cerebral blood flow in spinocerebellar degenerations: a single photon emission tomography study in 28 patients. J Neurol 1998;245:603–8.
[15] Klockgether T, Petersen D, Grodd W, Dichgans J. Early onset cerebellar ataxia with retained tendon reflexes. Clinical, electrophysiological and MRI observations in comparison with Friedreich's ataxia. Brain 1991;114:1559–73.

Acta Neurol Scand 2007: 116: 340–344 DOI: 10.1111/j.1600-0404.2007.00876.x

ACTA NEUROLOGICA
SCANDINAVICA

Constant blood flow reduction in premotor frontal lobe regions in ALS with dementia – a SPECT study with 3D-SSP

Ishikawa T, Morita M, Nakano I. Constant blood flow reduction in premotor frontal lobe regions in ALS with dementia – a SPECT study with 3D-SSP.
Acta Neurol Scand 2007: 116: 340–344.

Objectives – We investigated the regional cerebral blood flow in amyotrophic lateral sclerosis with dementia (ALS-D) patients, using single photon emission computed tomography (SPECT). *Materials and methods* – The ^{123}I-IMP SPECT data for 5 ALS-D and 16 ALS patients were analyzed using three-dimensional stereotactic surface projection (3D-SSP). *Results* – 3D-SSP demonstrated marked prefrontal hypoperfusion in all the five ALS-D cases and significant bilateral prefrontal hypoperfusion in group comparisons. *Conclusions* – This study revealed prefrontal hypoperfusion in ALS-D cases to be an obvious abnormality with scientific objectivity.

T. Ishikawa, M. Morita, I. Nakano

Division of Neurology, Department of Internal Medicine, Jichi Medical University, Tochigi, Japan

Key words: amyotrophic lateral sclerosis with dementia; premotor frontal lobe region; regional cerebral blood flow; single photon emission computed tomography; three-dimensional stereotactic surface projection

Mitsuya Morita, Division of Neurology, Department of Internal Medicine, Jichi Medical University, 3311-1 Yakushiji, Shimotsuke, Tochigi 329 0498, Japan
Tel.: +81 285 58 7352
Fax: +81 285 44 5118
e-mail: morita@jichi.ac.jp

Accepted for publication March 25, 2007

Introduction

Amyotrophic lateral sclerosis (ALS) is a degenerative disorder that involves progressive muscle weakness, and the lesions are essentially restricted to upper and lower motor neurons. Traditionally, patients with ALS have been recognized to be free from cognitive impairment. Evidence is emerging, however, that the cognitive function is impaired in some ALS patients, and such cases have been repeatedly described, especially in Japan (1).

Single photon emission computed tomography (SPECT) studies have been performed for the evaluation of the regional cerebral blood flow (rCBF) in various neurodegenerative disorders, including ALS and ALS-D. Such studies revealed cortical hypoperfusion in the premotor frontal lobe cortex and/or motor cortex in ALS (2, 3) or ALS with dementia (ALS-D) (4, 5), leading the researchers to state that ALS-D is included in the spectrum of ALS (6). The reported hypoperfusion in these regions, however, lacked objectivity, because the SPECT data were not standardized. With recent advances in computer-assisted analysis of SPECT images using three-dimensional stereotactic surface projection (3D-SSP) (7, 8), we have become able to detect a slight change in rCBF with scientific objectivity. Nevertheless, there have been few studies to discriminate subjects with ALS-D from non-demented ALS cases using such statistical methods. The purpose of this study was to evaluate rCBF in ALS-D and ALS cases using an objective and accurate method for analysis such as 3D-SSP, and to discuss the relationship between ALS-D and classic ALS.

Material and methods

Cases

Forty-one ALS cases had been diagnosed in the Neurology Department of Jichi Medical University from 1997 to 2003, five of whom had dementia. Among them, 16 ALS patients and five ALS with dementia patients could be evaluated by SPECT. Five ALS-D (two men and three women, mean ± SD: 54.8 ± 3.4 years old) and 16 ALS cases (nine men and seven women, mean ± SD: 66.5 ± 11.8 years old) were selected for analysis. The diagnosis of ALS was established according to the El Escorial criteria (9). None of the patients had either symptoms of a cerebrovascular disease or infarcts detectable in CT or MR images.

Table 1 Clinical features of the amyotrophic lateral sclerosis with dementia (ALS-D)

ALS-D cases	Age (years old) /Sex	The duration of illness at the time of SPECT (months)	Initial symptom	HDS-R	WAIS-R	Loss of memory	Insight into disease	Personality change /Emotional disorder	Autopsy
ALS-D 1	58/F	8	Memory loss	19	N/A	+	−	+	−
ALS-D 2	50/M	8	Memory loss	N/A	Verbal (57) Performance (51) Full (47)	+	−	+	+
ALS-D 3	59/F	19	Upper limb weakness	22	Verbal (100) Performance (75) Full (89)	−	−	+	+
ALS-D 4	52/F	27	Paranoia	18	N/A	+	−	+	+
ALS-D 5	55/M	45	Personality change	19	N/A	+	−	+	−
	54.8 ± 3.4 (mean ± SD)	21.4 ± 13.8 (mean ± SD)							
ALS cases									
Total 16 cases	66.5 ± 11.8 (mean ± SD)	21.4 ± 14.7 (mean ± SD)							

When individuals exhibited both ALS and an intellectual impairment constellation, such as loss of memory, personality change, emotional disorder and language impairment (the clinical features are summarized in Table 1), the diagnosis of ALS-D was made. For the evaluation of intellectual impairment, we used the Wechsler Adult Intelligence Scale-Revised (WAIS-R) and/or the revised Hasegawa Dementia Scale (HDS-R). The HDS-R is widely used as a brief cognitive screen instrument in Japan, and the result is known to be correlated well with the Mini-Mental State Examination (MMSE). The low-normal cut off is estimated to be 20, and the results are summarized in Table 1. Two ALS-D cases were also evaluated with the WAIS-R.

Assessment with the WAIS-R yielded a verbal IQ of 57, performance IQ of 51 and full IQ of 47 in case 2, a verbal IQ of 100, performance IQ of 75 and full IQ of 89 in case 3. Case 3 developed limb weakness as an initial symptom, and her intellectual impairment was negligible when she was diagnosed as having ALS, and SPECT study was carried out. Thereafter, she developed prominent dementia.

All the five ALS-D cases finally died of respiratory failure because of motor neuron involvement. Autopsy was performed in three cases (case 2, 3, and 4), and the diagnosis of ALS-D was confirmed according to the result of the autopsy. A total of 33 healthy volunteers (21 men and 12 women, mean ± SD: 58.6 ± 11.0 years old) was used as normal control subjects for 3D-SSP analysis.

SPECT and 3D-SSP

Single photon emission computed tomography with [^{123}I] isopropyl amphetamine (^{123}I-IMP SPECT) image sets was performed. The duration of illness at the time of SPECT was 21.4 ± 13.8 (mean ± SD) months in the ALS-D group and 21.4 ± 14.7 (mean ± SD) months in the ALS one, respectively. We performed 3D-SSP using the Neurological Statistical Image Analysis Software (NEUROSTAT) to evaluate the spatial distribution of an abnormal CBF, (8) and iSSP 35 for Windows to produce single subject *Z*-maps of decreased perfusion in patients. Following stereotactic anatomic standardization, the CBF in an individual's SPECT image set was extracted as a set of predefined surface pixels, which was used in the subsequent analysis. To quantify perfusion deficits, the normalized CBF in each patient was compared with that in 33 normal controls by pixel-by-pixel *Z*-score analysis ([normal mean]-[individual value])/(normal standard deviation; SD). We also compared the intergroup differences between the ALS-D group and normal controls, the ALS-D and ALS groups, and the ALS group and normal controls. A positive *Z*-score represents a reduced CBF in a patient relative to the control mean. In this study, we considered that a *Z*-score of >3.0 was significant.

Results

The statistical *Z*-scores obtained with 3D-SSP in the ALS-D patients are presented in the Fig. 1.

The reduction of rCBF was consistently prominent and widespread in the middle to inferior areas of the premotor frontal lobe in all five ALS-D patients, while the rCBF decrease in such regions was only subtle and patchy in ALS patients. A mild decrease in the unilateral temporal lobe was also seen in all the five ALS-D patients.

A significant rCBF reduction in the bilateral frontal lobes, especially the premotor frontal lobes,

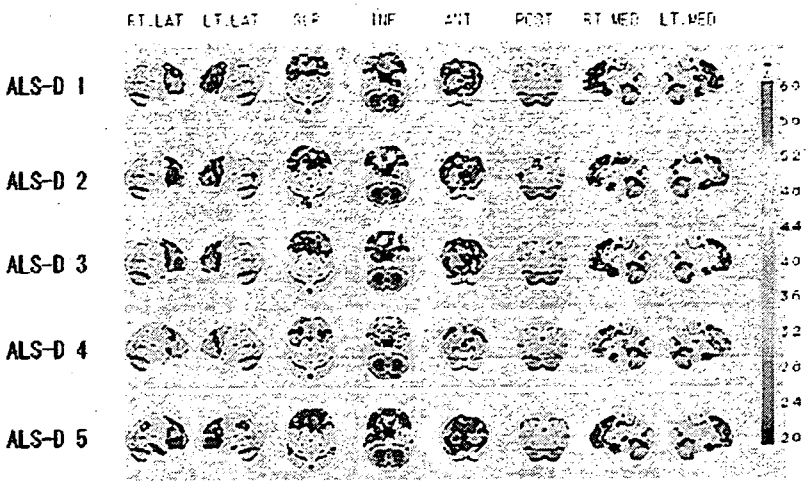

Figure 1. Three-dimensional stereotactic surface projection (3D-SSP) of the amyotrophic lateral sclerosis with dementia (ALS-D) cases compared with normal controls. The *Z*-score images obtained with 3D-SSP demonstrated marked regional cerebral blood flow reduction in the bilateral frontal lobes, especially the prefrontal lobes, in all five ALS-D patients. Images are constructed from eight views [in each line, from left to right, right lateral (RT. LAT), left lateral (LT. LAT), superior (SUP), inferior (INF), anterior (ANT), posterior (POST), right medial (RT. MED), and left medial (LT. MED)].

was evident in the ALS-D group compared with not only in normal controls but also in the ALS group (Fig. 2). One part of the left temporal lobe, the parahippocampal gyrus, also exhibited subtle hypoperfusion in the ALS-D group. On the contrary, in the ALS group, there were subtle rCBF decreases in the anterior part of the cingulate gyrus and the posterior part of the corpus callosum compared with in normal controls. Neither the ALS-D group nor the ALS one exhibited an obvious rCBF reduction in the regions corresponding to the precentral gyrus.

Discussion

Scintigraphical studies have been performed for the evaluation of rCBF in various neurodegenerative disorders, and some researchers have reported cortical hypoperfusion in the frontal cortex and motor cortex in ALS-D (4, 5). In the previous reports, however, as subjective approaches such as visual inspection were used, the reported hypoperfusion in these regions lacked objectivity. The 3D-SSP we used in this study is far superior to the visual inspection method in terms of objectivity. In addition, its sensitivity is reported to be high enough to be able to discriminate patients with a very early stage of the Alzheimer disease from healthy controls (7).

In our study, cortical hypoperfusion in the frontal lobe in the ALS-D group was consistently prominent compared to in the ALS cases, although the mean age of the ALS-D cases was lower than that of the controls or the ALS cases. CBF tends

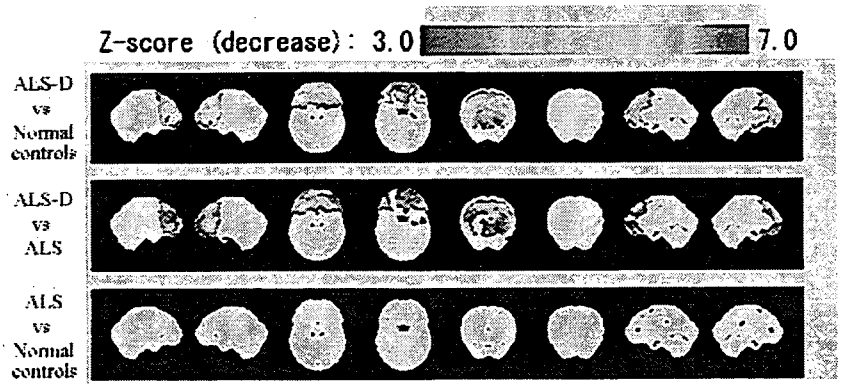

Figure 2. Decrease of regional cerebral blood flow (rCBF) adjusted to the global mean cerebral blood flow using three-dimensional stereotactic surface projection (3D-SSP) in group comparisons. 3D-SSP demonstrated a significant rCBF reduction in the bilateral frontal lobes, especially the prefrontal lobes, in the amyotrophic lateral sclerosis with dementia (ALS-D) group, when compared with either in normal controls or in the ALS group. On the contrary, subtle rCBF decreases in the anterior part of the cingulate gyrus and the posterior part of the corpus callosum were seen in the ALS group when compared with in normal controls. Images are constructed from 8 views in the same order as Fig. 1.

to be decreased in aged persons, so we might have underestimated the decrease in rCBF in the ALS-D group.

The change observed was notable in the inferolateral premotor frontal cortex in 4 of the 5 ALS cases, this being consistent with the previous results on ^{123}I-IMP SPECT and visual inspection (4, 5). This result is also supported by a previous neuropathological study on ALS-D that showed involvement of the inferomedial premotor frontal cortex, which is known to play important roles in emotional control and intellectual function (10). Thus, the decreased rCBF in the bilateral frontal lobe may play a role in the cognitive dysfunction in this condition.

In some of our ALS patients, a subtle reduction of rCBF in some parts of the frontal lobes, but strangely not in the precentral motor cortex, was observed, but the region was relatively restricted and variable. Our results are contrary to the findings in some previous studies (2, 3, 5) that revealed bilateral frontal hypoperfusion in ALS on visual inspection. In this study, no rCBF reduction was seen in the bilateral motor cortices not only in ALS-D but also in ALS. This result might indicate that there is actually no rCBF reduction in ALS, or we also need to consider the limit of sensitivity of this method.

What should we think about the relation between ALS and ALS-D? Most ALS-D cases reported previously shared characteristic neuropathological findings such as motor neuronal degeneration and Bunina bodies with classic/sporadic ALS. From the standpoint that ALS is a disease with widespread involvement of not only the pyramidal tract but also other systems, ALS-D belongs to the same clinical entity as ALS. However, the pattern of rCBF reduction in the ALS-D group in this study is apparently different from that of ALS, the pattern of ALS-D resembling that of fronto-temporal dementia (FTD). The hyporperfusion in the ALS-D group in this study could lead us to think that ALS-D is one form of FTD. However, most ALS-D cases reported previously had characteristic neuropathological findings consistent with sporadic ALS, such as Bunina bodies. It is essential that ALS-D is defined by supporting neuropathological investigation. If dementia is ultimately superimposed on ALS, the same decreasing rCBF pattern as in ALS-D should be observed in ALS cases, especially in ones with a long history. Actually, the most prominent rCBF reduction was observed in the case with the longest duration of the disease (45 months) among the ALS-D cases (case 5 of ALS-D). However, none of the 16 ALS cases showed the same pattern as that in ALS-D.

Furthermore, it is interesting that the cortical hypoperfusion in the frontal lobe was observed in one ALS-D case before the development of dementia. Case 3 with ALS-D developed limb weakness as an initial symptom, and at 19 months after the onset, ^{123}I-IMP SPECT was performed. Although the reduction of rCBF in the frontal lobe was obvious, her intellectual impairment was negligible at that time and became markedly worse after the examination. This suggests that a reduction of frontal rCBF could precede clinically evident dementia.

Based on our 3D-SSP analysis, it is reasonable to suppose that the pathogenesis of ALS-D is different from that of ALS, and 3D-SSP analysis might have a high predictive value for the diagnosis of ALS-D even at the stage of cryptic dementia.

There is the possibility that ALS-D may be overlooked, because ALS patients with severe bulbar symptoms tend to have trouble in verbal communication. We should always consider possible dementia hidden behind ALS, and recommend a SPECT study for ALS patients with any subtle signs and symptoms suggesting dementia.

Conclusion

Using 3D-SSP, we have demonstrated that ALS-D patients have a significantly reduced rCBF in the bilateral premotor frontal lobes compared with controls and ALS patients. The present study indicated that SPECT with 3D-SSP can clearly and objectively distinguish ALS-D from ALS. This finding seems to be useful for the diagnosis of ALS-D even at an early stage of dementia. A decreased rCBF in the bilateral premotor frontal lobes may be associated with dementia in ALS-D patients and help us to recognize the pathogenesis of the disease.

Acknowledgements

The authors are very grateful to Mr Y. Kawamura for providing the cases for the SPECT database, and to Mr M. Suzuki for the skilful editing.

References

1. Mitsuyama Y. Presenile dementia with motor neuron disease in Japan: clinico-pathological review of 26 cases. J Neurol Neurosurg Psychiatry 1984;47:953–9.
2. Abe K, Fujimura H. Single-photon emission computed tomographic investigation of patients with motor neuron disease. Neurology 1993;43:1569–73.
3. Waldemar G, Vorstrup S. Focal reductions of cerebral blood flow in amyotrophic lateral sclerosis: a [^{99m}Tc]-*d,l*-HMPAO SPECT study. J Neurol Sci 1992;107:19–28.

4. Neary D, Snowden JS. Frontal lobe dementia and motor neuron disease. J Neurol Neurosurg Psychiatry 1990;53: 23–32.
5. Vercelletto M, Ronin M. Frontal type dementia preceding amyotrophic lateral sclerosis: a neuropsychological and SPECT study of five clinical cases. Eur J Neurol 1999;6:295–9.
6. Talbot PR, Goulding PJ. Inter-relation between 'classic' motor neuron disease and frontotemporal dementia: neuropsychological and single photon emission computed tomography study. J Neurol Neurosurg Psychiatry 1995;58:541–7.
7. Imabayashi E, Matsuda H. Superiority of 3-dimensional stereotactic surface projection analysis over visual inspection in discrimination of patients with very early Alzheimer's disease from controls using brain perfusion SPECT. J Nucl Med 2004;45:1450–7.
8. Minoshima S, Frey KA. A diagnostic approach in Alzheimer's disease using three-dimensional stereotactic surface projections of fluorine-18-FDG PET. J Nucl Med 1995;36: 1238–48.
9. Brooks BR. El Escorial World Federation of Neurology criteria for the diagnosis of amyotrophic lateral sclerosis. Subcommittee on Motor Neuron Diseases/Amyotrophic Lateral Sclerosis of the World Federation of Neurology Research Group on Neuromuscular Diseases and the El Escorial 'Clinical limits of amyotrophic lateral sclerosis' workshop contributors. J Neurol Sci 1994;124:(Suppl.): 96–107.
10. Abe K, Fujimura H. Cognitive function in amyotrophic lateral sclerosis. J Neurol Sci 1997;148:95–100.

Reversible limbic encephalitis with antibodies against the membranes of neurones of the hippocampus

H Shimazaki, Y Ando, I Nakano and J Dalmau

J. Neurol. Neurosurg. Psychiatry 2007;78;324-325
doi:10.1136/jnnp.2006.104513

PostScript

LETTERS

Reversible limbic encephalitis with antibodies against the membranes of neurones of the hippocampus

Paraneoplastic limbic encephalitis (PLE) is a rare neurological syndrome characterised by short-term memory impairment, seizures and various psychiatric disturbances. It is often associated with small-cell lung cancer, germ-cell tumours of the testis and breast cancer, but rarely with ovarian teratoma.[1] Several cases of PLE with ovarian teratoma have been reported, but the autoantigens of this disease remain unknown. Recently, an antibody to the membranes of neurones of the hippocampus (antigens colocalising with exchange factor for ADP-ribosylation factor 6 A (EFA6A)) was reported in association with PLE and ovarian teratoma.[2] Here, we report a case of a young Japanese woman who had PLE with ovarian teratoma, and whose serum and cerebrospinal fluid (CSF) contained an antibody against the membranes of neurones of the hippocampus. Immunosuppressive treatments resulted in a rapid improvement.

A 30-year-old woman was admitted to our hospital (Jichi Medical University, Tochigi, Japan) in April 2004 because of headache, fever and disorientation for 3 days. Figure 1A summarises the clinical course of the patient. She had no relevant family or medical history of interest. Her temperature was 37.8°C. Neurological examination on admission showed only recent memory disturbance. Examination of CSF showed increased protein concentration (670 mg/l), an increased number of mononuclear-dominant cells (40/mm^3) and 67 mg/dl glucose. CSF cytology was negative for malignant cells. Polymerase chain reaction for herpes simplex virus (HSV) was negative. No marked increase in anti-HSV, varicella zoster virus, human herpes virus type 6, cytomegalovirus or Epstein–Barr virus antibodies was detected in a paired CSF sample. Anti-toxoplasma and Japanese encephalitis virus antibodies were negative in the serum. The serum did not contain increased anti-nuclear, double-strand DNA, SS-A or thyroid antibodies. Anti-Yo, anti-Hu, anti-Ri, anti-CV2 (CRMP-5), anti-Tr, anti-Ma-2 and amphyphysin antibodies were negative in serum and CSF. Anti-voltage-gated potassium channel antibodies were not detected. Although axial plane and gadolinium-enhanced T1-weighted magnetic resonance images (MRI) were unremarkable, T2-weighted and fluid-attenuated inversion recovery images showed areas of mild hyperintensity in bilateral medial temporal lobes and hippocampus (fig 1B); these abnormalities had resolved by the time of the follow-up study in June 2004 (fig 1C).

Initial treatments included methylprednisolone (1000 mg/day for 3 days) and aciclovir (1500 mg/day). This treatment was associated with mild and transient decrease of fever, but tonic convulsions, disturbance of consciousness, restlessness and anxiety emerged and became worse. The electroencephalogram showed diffuse δ–θ waves. These symptoms and hypoventilation led to her being sedated and on a mechanical ventilator for 6 weeks with anticonvulsant treatment. Anisocoria, skew deviation and involuntary movement, such as epilepsia partialis continua, were observed for 2 weeks. Several attempts to wean the patient from the ventilator and decrease the sedation resulted in exacerbation of the involuntary movements and hypoventilation. Subsequently, the patient was treated with plasmapheresis (three exchanges) and intravenous immunoglobulin (400 mg/kg/day) for 5 days. The fever and convulsions began to subside about 4 weeks after her admission. She

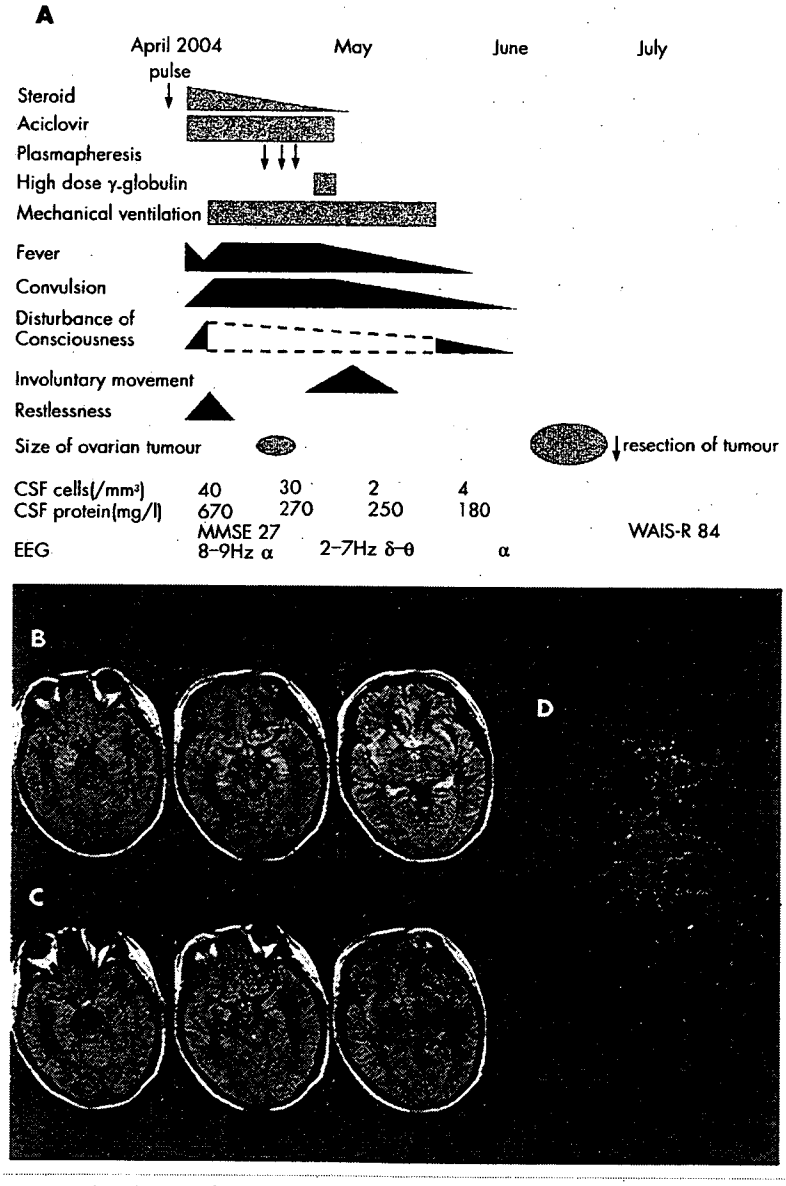

Figure 1 Clinical course of the patient, magnetic resonance image of the brain and immunolabelling of live rat hippocampal neurones with the patient's cerebrospinal fluid (CSF). (A) Clinical course of the patient. The symptoms and laboratory data were improved before the tumour resection. (B) MRI fluid-attenuated inversion recovery images of the brain in April 2004 showed areas of hyperintensity in the medial temporal lobes, cingulate gyrus, insular regions and hippocampus. (C) These abnormalities had resolved by June 2004. (D) The patient's antibodies, which colocalised with EFA6A, showed intense immunolabelling of the neuronal cell membranes and processes, using methods previously reported[2]. WAIS-R, Weschler Adult Intelligence Scale—Revised.

could breath spontaneously and all CSF studies became normal in May 2004.

In April 2004, an abdominal computed tomography had shown a 5 cm tumour in the right ovary, which was considered a benign cyst unrelated to the neurological disorder. In June 2004, the patient developed progressive constipation and a bulging appearance of the lower abdomen. Follow-up abdominal computed tomography and MRI showed an enlarged ovarian tumour, with a transverse diameter of 10 cm. On 28 June, resection of the tumour showed an immature teratoma that contained hair follicles, cartilage tissue, glandular structures and cerebral cortex-like tissue with normal appearing neurones. No inflammatory infiltrates were evident in the tumour.

Although her Wechsler Adult Intelligence Scale—Revised score was 84, she recovered and exhibited no limitations in activity of daily living in July 2004. After she was discharged from our hospital in July, she received ambulatory neurocognitive rehabilitation. She refused follow-up Wechsler Adult Intelligence Scale—Revised, but otherwise the cognitive functions and electroencephalogram appeared normal. She returned to her job as a medical resident in April 2005.

Analysis of the patient's serum and CSF showed antibodies, colocalised with EFA6A, which predominantly reacted with the neuropil of the hippocampus and cell membrane of rat hippocampal live neurones (fig 1D).

Discussion

We consider that this patient had definite paraneoplastic encephalitis, with predominant involvement of the limbic system. Accordingly, she developed subacute onset of short-term memory loss, seizures, psychiatric symptoms, CSF pleocytosis, MRI abnormalities in the limbic system and antineural antibodies.[3] Central nervous system tissue in the teratoma might be a trigger of the immune reaction. Central hypoventilation, skew deviation and anisocoria were observed during the most critical period. These symptoms suggest the involvement of her brain stem.

Previous reports of paraneoplastic encephalitis and ovarian teratoma showed MRI abnormalities in the frontal cortex, cerebellum and brain stem, but no case exhibited the characteristic medial temporal abnormalities observed in our patient.[2 4] This finding might have resulted from hippocampal inflammation related to the immune response predominantly reacting with hippocampal neurones.

Most patients with PLE and ovarian teratoma improved with resection of the teratomas.[2 4] We discovered the tumour in our patient 2 weeks after presentation of the encephalitis, but the benign appearance of the tumour and her poor physical status did not prompt for tumour resection. Instead, we started treatment with corticosteroids, plasmapheresis and intravenous immunoglobulin, and she began to improve before the tumour resection. This finding suggests that immunotherapy may provide the improvement needed to undergo the procedure for patients whose poor clinical condition prevents surgery. Furthermore, our patient began to recover faster (4 weeks after admission) than any other reported cases (7–16 weeks).[2] We presumed that this faster improvement resulted from the combination of immunotherapies. Immunocytochemistry with rat hippocampal live neurones showed the presence of antibodies to antigens present in the neuronal cell membranes and processes and colocalised with EFA6A, as previously reported.[2] The surface localisation of the autoantigen might be one reason for the effectiveness of these immunotherapies.[5]

PLE with ovarian teratoma has a better prognosis than that associated with other tumours.[2] Prompt detection of antibodies that colocalise with EFA6A is useful in predicting a clinical response to immunotherapy and tumour resection and a favourable outcome despite the severity of the disorder.

Acknowledgements

We thank Dr Keiko Tanaka, Department of Neurology, Brain Research Institute, Niigata University, and Dr Yukitoshi Takahashi, Department of Pediatrics, National Epilepsy Center, Shizuoka Institute of Epilepsy and Neurological Disorders, for measurement of the anti-neuronal antibodies.

H Shimazaki, Y Ando, I Nakano
Division of Neurology, Department of Internal Medicine, Jichi Medical University, Tochigi, Japan

J Dalmau
Division of Neuro-Oncology, Department of Neurology, University of Pennsylvania, Pennsylvania, USA

Correspondence to: Dr H Shimazaki, Division of Neurology, Department of Internal Medicine, Jichi Medical University, Tochigi 329-0498, Japan; hshimaza@jichi.ac.jp

Informed consent was obtained from the patient for publication of the features of the case.

doi: 10.1136/jnnp.2006.104513

Funding: This work was supported by a Jichi Medical University Young Investigator Award.

Competing interests: None.

References

1 **Gultekin SH**, Rosenfeld MR, Voltz R, *et al.* Paraneoplastic limbic encephalitis: neurological symptoms, immunological findings and tumour association in 50 patients. *Brain* 2000;**123**:1481–94.
2 **Vitaliani R**, Mason W, Ances B, *et al.* Paraneoplastic encephalitis, psychiatric symptoms, and hypoventilation in ovarian teratoma. *Ann Neurol* 2005;**58**:594–604.
3 **Graus F**, Delattre JY, Antoine JC, *et al.* Recommended diagnostic criteria for paraneoplastic neurological syndromes. *J Neurol Neurosurg Psychiatry* 2004;**75**:1135–40.
4 **Koide R**, Shimizu T, Koike K, *et al.* EFA6A-like antibodies in paraneoplastic encephalitis associated with immature ovarian teratoma: a case report. *J Neuro-Oncol.* In press.
5 **Darnell RB**, Posner JB. A new cause of limbic encephalopathy. *Brain* 2005;**128**:1745–6.

Devic's syndrome-like phenotype associated with thymoma and anti-CV2/CRMP5 antibodies

The case of a patient who presented with a necrotic myelopathy and bilateral optic neuritis in association with a thymoma and circulating anti-CV2/CRMP5 antibodies is reported. This case shows that in some rare instances, a clinical presentation suggestive of a neuromyelitis optica can be of paraneoplastic origin.

A 45-year-old woman with a history of Hashimoto thyroiditis presented with a 4-month history of asthenia and a weight loss of 10 kg. A computed tomography of the chest showed an anterior mediastinal mass suspicious for a thymoma. The mediastinal mass was completely removed by surgery. Histological examination showed a B2-type thymoma with pleural, pericardial and left phrenic local extension. There was no evidence of mediastinal adenopathy or metastasis on computed tomography of the abdomen and pelvis. Treatment with radiation therapy was planned, but 1 month later the patient developed difficulties in walking for over 2 weeks, paraesthesia of the four limbs and bladder dysfunction.

Neurological examination showed a left spastic motor paresis, brisk reflexes and a left Babinski response; proprioceptive sensation was predominantly affected on the left limbs, whereas pain and thermal sensation were affected on the right limbs, suggesting a left cervical Brown-Sequard syndrome. Visual acuity was initially normal. There was no sign of polyneuropathy, and electromyography was normal. The patient did not have fever, and had no signs of systemic disease and no sicca syndrome on general examination. Magnetic resonance imaging (MRI) of the spine showed an enlargement of the cervical cord consecutive to an extensive cervicodorsal (C1 to D7) intramedullary lesion with focal heterogenous gadolinium enhancement (fig 1A,B). MRI of the brain was normal. The cerebrospinal fluid (CSF) had only an increased protein concentration of 82 g/dl; there was no intrathecal synthesis of IgG, and isoelectric focusing was negative. Polymerase chain reaction of herpes simplex virus (HSV)1 and HSV2 was negative in the CSF on two occasions. The following microbiological tests were also negative; enterovirus, varicella zoster virus, cytomegalovirus, Epstein-Barr virus, Lyme disease, syphilis, HIV and *Mycoplasma pneumoniae*. Anti-double-stranded DNA antibodies and anti-Sjogren's syndrome A and B antibodies were negative.

As an intramedullary metastasis of the thymoma was suspected, a biopsy of the lesion was performed at level C7. On histological examination, the lesions were found to be localised in both white and and grey matter. These lesions consisted of a reactive gliosis, with foci of oedema and necrosis with numerous macrophages and some perivascular lymphocytes (fig 1C,D). Bodian luxol coloration showed demyelinisation. There were no features of vasculitis, nor of viral inclusion or tumour infiltration. This was consistent with a necrotic myelopathy. Serum screening for neuromyelitis optica (NMO) IgG antibodies was negative.[1] Serum screening for onconeural antibodies was negative for anti-Hu, anti-Ri, anti-Yo, and anti-amphyphysin antibodies, but was strongly positive for anti-CV2/CRMP5 antibodies. Immediately after the biopsy, the patient became quadripleglic; this deterioration was probably related to the biopsy. She developed an intestinal subocclusion complicated with aspiration pneumonia. She was treated with high-dose methylprednisolone, but her condition did not improve and she developed a respiratory insufficiency that necessitated artificial ventilation in an intensive care unit. Ten plasma exchanges were also ineffective. At 4 months after the onset of myelopathy, the patient presented a bilateral painless visual loss. Funduscopic examination was normal, and evoked visual potentials showed a bilateral optic neuropathy. The patient finally died of septicaemia 5 months after the onset of myelopathy. No necropsy was performed.

Circulation Research

JOURNAL OF THE AMERICAN HEART ASSOCIATION

American Heart Association®

Learn and Live℠

Interleukin-10 Expression Mediated by an Adeno-Associated Virus Vector Prevents Monocrotaline-Induced Pulmonary Arterial Hypertension in Rats

Takayuki Ito, Takashi Okada, Hiroshi Miyashita, Tatsuya Nomoto, Mutsuko Nonaka-Sarukawa, Ryosuke Uchibori, Yoshikazu Maeda, Masashi Urabe, Hiroaki Mizukami, Akihiro Kume, Masafumi Takahashi, Uichi Ikeda, Kazuyuki Shimada and Keiya Ozawa

Circ. Res. 2007;101;734-741; originally published online Aug 2, 2007;
DOI: 10.1161/CIRCRESAHA.107.153023
Circulation Research is published by the American Heart Association. 7272 Greenville Avenue, Dallas, TX 72514
 Print ISSN: 0009-7330. Online ISSN: 1524-4571

Interleukin-10 Expression Mediated by an Adeno-Associated Virus Vector Prevents Monocrotaline-Induced Pulmonary Arterial Hypertension in Rats

Takayuki Ito, Takashi Okada, Hiroshi Miyashita, Tatsuya Nomoto, Mutsuko Nonaka-Sarukawa, Ryosuke Uchibori, Yoshikazu Maeda, Masashi Urabe, Hiroaki Mizukami, Akihiro Kume, Masafumi Takahashi, Uichi Ikeda, Kazuyuki Shimada, Keiya Ozawa

Abstract—Pulmonary arterial hypertension (PAH) is a fatal disease associated with inflammation and pathological remodeling of the pulmonary artery (PA). Interleukin (IL)-10 is a pleiotropic antiinflammatory cytokine with vasculoprotective properties. Here, we report the preventive effects of IL-10 on monocrotaline-induced PAH. Three-week-old Wistar rats were intramuscularly injected with an adeno-associated virus serotype 1 vector expressing IL-10, followed by monocrotaline injection at 7 weeks old. IL-10 transduction significantly improved survival rates of the PAH rats 8 weeks after monocrotaline administration compared with control gene transduction (75% versus 0%, $P<0.01$). IL-10 also significantly reduced mean PA pressure (22.8 ± 1.5 versus 29.7 ± 2.8 mm Hg, $P<0.05$), a weight ratio of right ventricle to left ventricle plus septum (0.35 ± 0.04 versus 0.42 ± 0.05, $P<0.05$), and percent medial thickness of the PA ($12.9\pm0.3\%$ versus $21.4\pm0.4\%$, $P<0.01$) compared with controls. IL-10 significantly reduced macrophage infiltration and vascular cell proliferation in the remodeled PA in vivo. It also significantly decreased the lung levels of transforming growth factor-β_1 and IL-6, which are indicative of PA remodeling. In addition, IL-10 increased the lung level of heme oxygenase-1, which strongly prevents PA remodeling. In vitro analysis revealed that IL-10 significantly inhibited excessive proliferation of cultured human PA smooth muscle cells treated with transforming growth factor-β_1 or the heme oxygenase inhibitor tin protoporphyrin IX. Thus, IL-10 prevented the development of monocrotaline-induced PAH, and these results provide new insights into the molecular mechanisms of human PAH. (***Circ Res.*** **2007;101:734-741.)**

Key Words: pulmonary hypertension ■ interleukins ■ gene therapy ■ inflammation ■ vascular smooth muscle cell proliferation

Pulmonary arterial hypertension (PAH) is an intractable disease that leads to increased pulmonary arterial pressure, progressive right heart failure, and premature death; however, no satisfactory treatment for PAH has been established.[1] The pathological process of PAH is characterized by abnormal remodeling of the pulmonary artery (PA) associated with excessive proliferation of pulmonary arterial smooth muscle cells (PASMCs).[2] Accumulating evidence suggests important roles of vascular inflammation in its pathogenesis.[2,3] For instance, serum levels of proinflammatory cytokines such as interleukin (IL)-1 and IL-6 reflect the disease activity in patients with idiopathic PAH.[4] Furthermore, injection of IL-6 can produce PAH and PA remodeling in rats.[5] The remodeled PA presents macrophage infiltration and increased expression of a variety of cytokines, including IL-6, tumor necrosis factor (TNF)-α, and transforming growth factor (TGF)-β_1.[6,7] Administration of steroids or immunosuppressive drugs decreases the level of PA pressure in patients with PAH.[8,9] These observations suggest a therapeutic potential of targeting inflammation to prevent PAH progression.[10] However, the precise mechanisms underlying the antiinflammatory effects on PA remodeling have not yet been fully investigated.

IL-10 is a multifunctional antiinflammatory cytokine with a vasculoprotective property. During the course of inflammation, IL-10 is produced by type-2 helper T (Th2) lymphocytes, and it inhibits the production of various proinflammatory cytokines in macrophages and Th1 lymphocytes.[11] Exogenous IL-10 prevents proliferative vasculopathy in vivo by inhibiting inflammatory cell infiltration,[12] smooth muscle cell proliferation,[12,13] and chemokine expression.[14] However, clinical efficacy of systemic recombinant IL-10 administra-

Original received March 28, 2007; revision received July 12, 2007; accepted July 23, 2007.

From the Division of Genetic Therapeutics (T.I., T.N., M.N.-S., M.U., H.M., A.K., K.O., R.U.), the Division of Cardiovascular Medicine (T.I., H.M., M.N.-S., K.S., Y.M.), Jichi Medical University, Japan; the Department of Molecular Therapy (T.O.), National Institute of Neuroscience, National Center of Neurology and Psychiatry, Japan; and the Department of Organ Regeneration (M.T., U.I.), Shinshu University Graduate School of Medicine, Japan.

Correspondence to Takayuki Ito, MD, PhD, Division of Genetic Therapeutics, Jichi Medical University, 3311-1 Yakushiji, Shimotsuke, Tochigi 329-0498, Japan. E-mail titou@jichi.ac.jp

Circulation Research is available at http://circres.ahajournals.org

DOI: 10.1161/CIRCRESAHA.107.153023

tion are insufficient because of the lower local IL-10 levels resulting from its short bioactive half-life.[15] In this study, we used an adeno-associated virus (AAV) vector for IL-10 expression because it is an efficient vehicle for systemic and sustained expression of therapeutic proteins.[14] It also has an advantage over other viral vectors in the therapeutic or mechanistic analysis because it produces minimal inflammatory and immune responses in vivo.

Recently, heme oxygenase (HO)-1, an inducible form of HO that promotes production of a vasodilator carbon monoxide (CO), was shown to mediate antiinflammatory and antiproliferative effects of IL-10 in a model of chronic vasculopathy.[12] Increased HO-1 and CO levels attenuated PAH and PA remodeling by inhibiting PASMC proliferation.[16–18] However, no study has explored a direct link between IL-10 and HO-1 in the pathogenesis of PAH. Thus, we examined the effects of IL-10, delivered via an AAV vector, on PA remodeling in a widely-used rat model of PAH induced by the pyrolizidine alkaloid monocrotaline (MCT). We also investigated the mechanisms underlying the effects of IL-10 on the following factors involved in the inflammatory and proliferative vascular changes in PAH: PASMC, macrophage, TGF-β_1, IL-6, and HO-1.

Materials and Methods

AAV Vector Production

DNA encoding rat IL-10 was polymerase chain reaction-amplified from rat splenocyte complementary DNA, using the primers 5′-GCACGAGAGCCACAACGCA-3′ and 5′-GATTTGAGTACG-ATCCATTTATTCAAAACGAGGAT-3′. For efficient transgene expression in the skeletal muscle, we constructed a recombinant AAV vector which carried the IL-10 gene (AAV-IL-10) or enhanced green fluorescent protein (eGFP) gene (AAV-eGFP), controlled by the modified chicken β-actin promoter with the cytomegalo virus-immediate early enhancer and the woodchuck hepatitis virus post-transcriptional regulatory element (a kind gift from Dr Thomas Hope, Infectious Disease Laboratory, Salk Institute). AAV vectors were prepared according to the previously described 3-plasmid transfection adenovirus-free protocol with minor modifications to use the active gassing system.[19,20] In brief, 60% confluent human embryonic kidney 293 cells incubated in a large culture vessel with active air circulation were cotransfected with the proviral transgene plasmid, AAV-1 chimeric helper plasmid (p1RepCap), and adenoviral helper plasmid pAdeno (Avigen Inc). The crude viral lysate was purified by 2 rounds of cesium chloride 2-tier centrifugation.[21] The viral stock titer was determined against plasmid standards by dot blot hybridization, after which the stock was dissolved in HN buffer (50 mmol/L HEPES, pH 7.4, 0.15 mol/L NaCl) before injection.

Animal Models

All animal experiments were approved by the Jichi Medical University ethics committee and were performed in accordance with the *National Institute of Health Guide for the Care and Use of Laboratory Animals*. To evaluate the efficiency of in vivo gene expression, 3-week-old male Wistar rats (Clea Japan Inc, Tokyo, Japan) weighing 45 to 55 g were injected with AAV-IL-10 (200 μL, 3×10^{10} to 1×10^{11} genome copies [g.c.] per body) into the bilateral anterior tibial muscles (n=3 animals per group). For hemodynamic and histological analysis, we randomly formed 4 groups comprising 5 rats each: sham rats that were administered the HN buffer (1, NC group); MCT-treated rats administered the HN buffer (2, MCT group); MCT rats administered AAV-eGFP (3, MCT+eGFP group); and MCT rats administered AAV-IL-10 (4, MCT+IL-10 group). After anesthetized with a spontaneous inhalation of 1% isoflurane, the rats in the groups 3 and 4 received intramuscular injection of AAV-eGFP or AAV-IL-10 (200 μL, 6×10^{10} g.c. per body), respectively. Rats in groups 1 and 2 were injected with the HN buffer (200 μL). MCT (Wako Pure Chemicals) was dissolved in 0.1N HCl, and the pH adjusted to 7.4 with 1.0N NaOH. For hemodynamic and histological studies, all rats except those in the NC group were subcutaneously injected with MCT (30 mg/kg) under the spontaneous inhalation of 1% isoflurane at 4 weeks after vector treatment. For the survival study, rats (n=8 animals/group) were injected with a lethal dose of MCT (45 mg/kg) under the spontaneous inhalation of 1% isoflurane at 4 weeks after vector injection. Survival was estimated from the date of MCT injection until death or 8 weeks after injection.

Hemodynamic Analysis

Four weeks after MCT injection, the rats were anesthetized with spontaneous inhalation of 1% isoflurane, and a tracheotomy was performed. Then, they were mechanically ventilated using a respirator (SAR-830/AP, CWE; tidal volume: 10 mL/kg, respiratory rate: 30 breaths per min) and anesthetized with 0.5% isoflurane through a tracheostomy. After the thoracic cavity was opened using a midsternal approach, 2.0F high-fidelity manometer-tipped catheters (SPC-320, Millar Instruments Inc) were inserted directly into the right or left ventricle. The mean pulmonary arterial pressure (mPAP) or mean aortic arterial pressure (mAoP) was measured using the catheters that were advanced from the right or left ventricle, respectively. The heart rate (HR) was measured by unipolar lead electrocardiography.

Ventricular Weight Measurement and Morphometric Analysis of the PA

After hemodynamic analysis, the rats were euthanized using an overdose isoflurane (5%). The lungs and PAs were perfused with 5 mL of saline followed by 10 mL of cold 4% paraformaldehyde. Each ventricle and the lungs were excised, dissected free, and weighed. The weight ratio of right ventricle to the left ventricle plus septum [RV/(LV+S)] was calculated as an index of right ventricular hypertrophy (RVH). The tissues were fixed in 4% paraformaldehyde for 4 hours, transferred to 30% sucrose in 0.1 mol/L phosphate buffer (pH 7.4) for cryoprotection, and stored at 4°C overnight. Lung tissue was frozen in Tissue-Tek OCT compound (Sakura Finetechnical Co) at −20°C. Then, 7-μm sections were cut using a cryostat. Hematoxylin and eosin (HE) staining was performed on sections from the middle lobe of the right lung, and these were examined using light microscopy. Morphometric analysis was performed in PAs with an external diameter of 25 to 50 and 51 to 100 μm. The medial wall thickness was calculated with the following formula: medial thickness (%)=medial wall thickness/external diameter×100.[22] For quantitative analysis, 30 vessels from each rat were counted and the average was calculated.

Immunohistochemistry

Immunohistochemical staining was performed with monoclonal antibodies against ED1 (1:100; Serotec) and proliferating cell nuclear antigen (PCNA, 1:200; Zymed), using the streptavidin-biotin-peroxidase method, as described previously.[23] ED1 recognizes the lysosomal membrane antigen expressed by a majority of tissue macrophages. Irrelevant mouse immunoglobulin G (Vector Laboratories) was used as a negative control. Reactions were visualized using Vector SG (Vector Laboratories) or 3,3′-diaminobenzidine (Zymed) and counterstained with nuclear fast red or hematoxylin. The number of ED1-positive cells was counted in 250×250-μm fields under 400× magnification and expressed as cells per mm^2. The number of PCNA-positive cells was quantitatively evaluated as a percentage of total vascular cells in the fields under 1000× magnification. For each rat, the average number or percentage of each cell in 15 randomly selected fields was used for statistical analysis.

Protein Assay

Protein samples were prepared by homogenization of the frozen lung tissue in lysis buffer [10 μmol/L Tris/Cl (pH 8.0), 0.2% NP-40,